

## ABSTRACT

The flux-coupling type superconducting fault current limiter (FC-SFCL) is suggested to suppress the surge current in ac and dc power systems. One FC-SFCL module with two branches is designed and tested. For the FC-SFCL module, the two branches could use the same or different YBCO tapes. Furthermore the electromagnetic analysis and parameter calculation of the module are performed. In order to study the current-limiting performance of the FC-SFCL under the rapid change of fault current, a dynamic simulation model is established. Finally, the transient properties of FC-SFCL module are simulated and tested.

## INTRODUCTION

- In current SFCL technology, the resistive SFCL is widely concerned because of its simplicity and good current limiting characteristics.
- For large-capacity resistive SFCL, the design of non-inductive coil is one of its key technologies. The pancake type has the merit in terms of compactness, AC loss, and current limiting performance, whereas weakness of insulation and mechanical/thermal stability.
- Compared with the bifilar pancake coil, the series solenoid coils also suffered that the full coil voltage exists between adjacent outlet end turns. In addition, the mechanism of fault suppression is lack for conventional resistive SFCL modules, if one unit is destructed in current limiting and reclosing process, the chain reaction will occur, resulting in the destruction of the parallel component.
- The parallel solenoid coil structure has high voltage insulation port easy to control, and good thermal stability, but detailed circuit topology and winding configuration was not given.

## GENERAL DESIGN OF FC-SFCL MODULE

- For the FC-SFCL module, both the inner and outer coils adopt solenoid structure.
- The windings are wound with Type 8602 YBCO tapes supplied by AMSC, the measured critical current is larger than 260 A at self-field and 77 K.
- The total impedance of coil assembly is related to the quench resistance and inductance of each branch, and the mutual inductance between the branches.

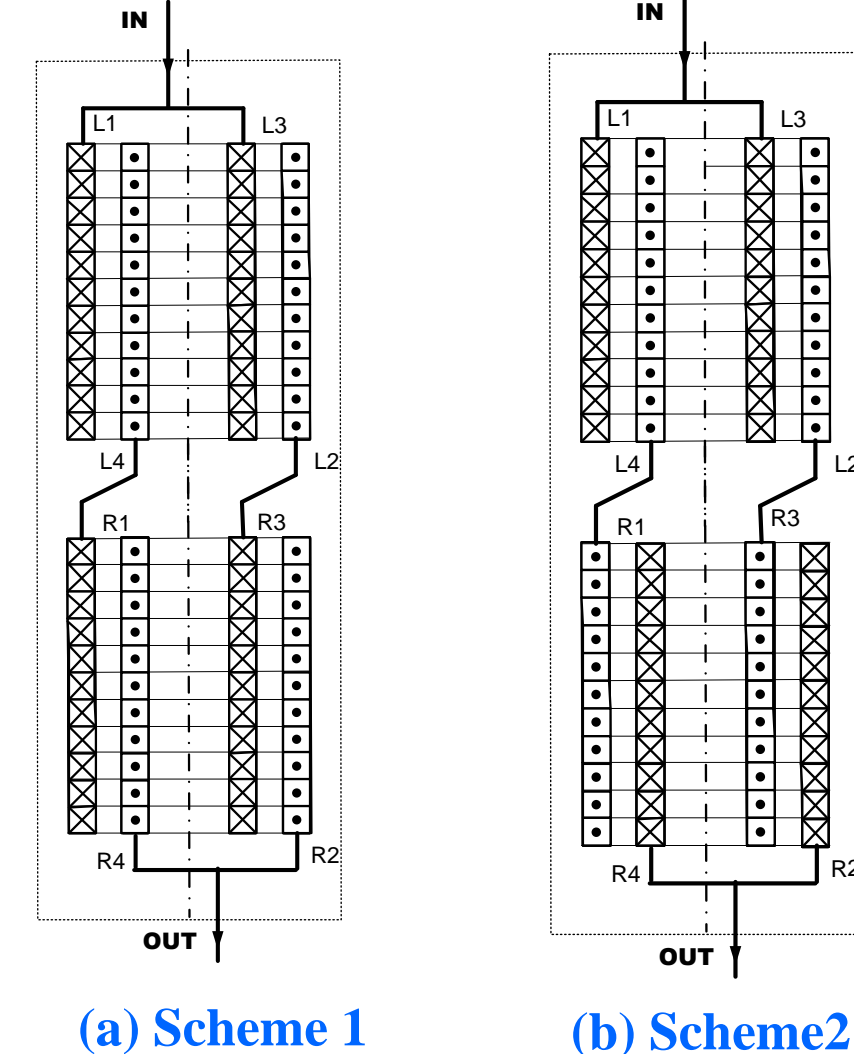


Fig. 1. Winding and connection styles of one FC-SFCL module.

TABLE I Specification of one FC-SFCL module

Parameters	Designed value
Number of parallel branches	2
Number of series branches	2
Number of coil	4
Diameter of one solenoid coil / mm	216 (IN) ; 176 (OUT)
Number of turns of one solenoid coil	28
Hight of one solenoid coil / mm	420
Thickness of interturn insulation / mm	1.5
Total hight of SFCL module / mm	900
Length of tapes / m	70
Operating temperature / K	65-77
Terminal voltage / kV	8
Resistance at room temperature / $\Omega$	2
Critical current / A	400@77 K; 800@65 K

TABLE III Inductance of one FC-SFCL module

	Scheme 1	Scheme 2
Leakage Inductance / $\mu\text{H}$	8.23	8.15
Self Inductance / $\mu\text{H}$	120.55	128.24

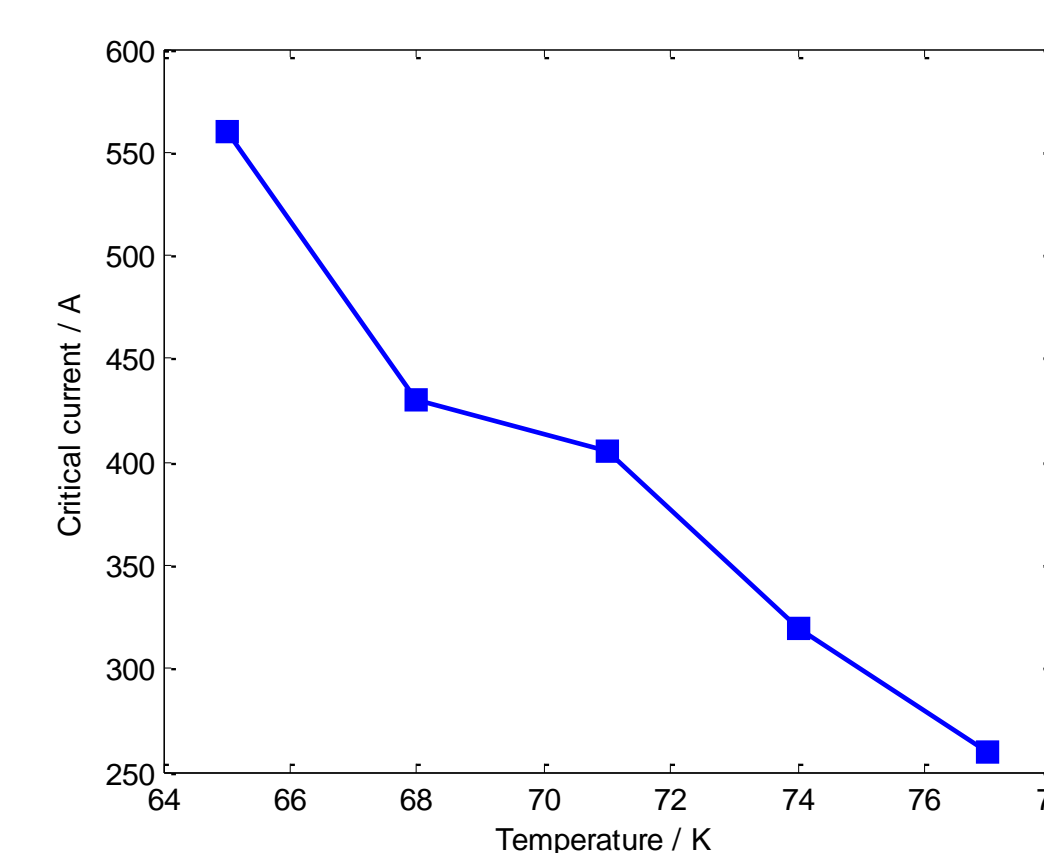


Fig. 2.  $I_c$ -temperature curve of AMSC 8602.

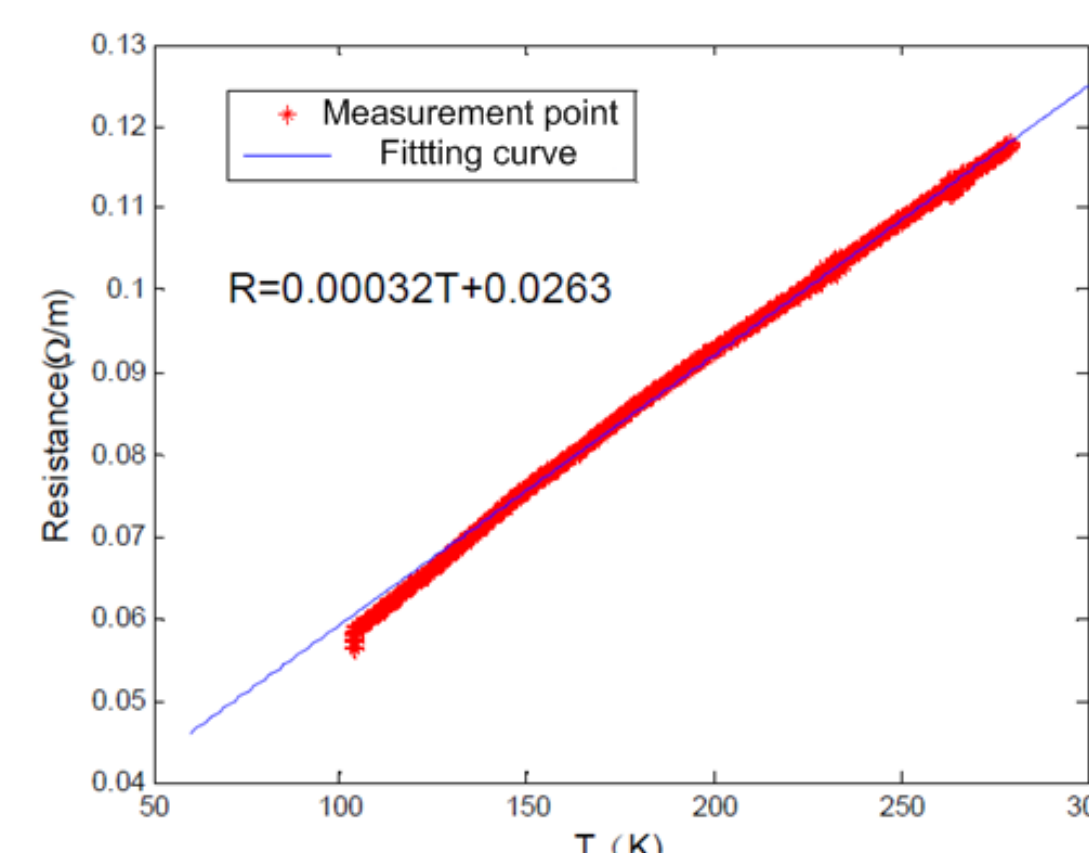


Fig. 3. Resistance-temperature curve of AMSC 8602.

## MAGNETIC FIELD ANALYSIS OF SFCL MODULE

- The magnetic field and inductance of the one solenoid group are simulated via 2D finite element simulation.

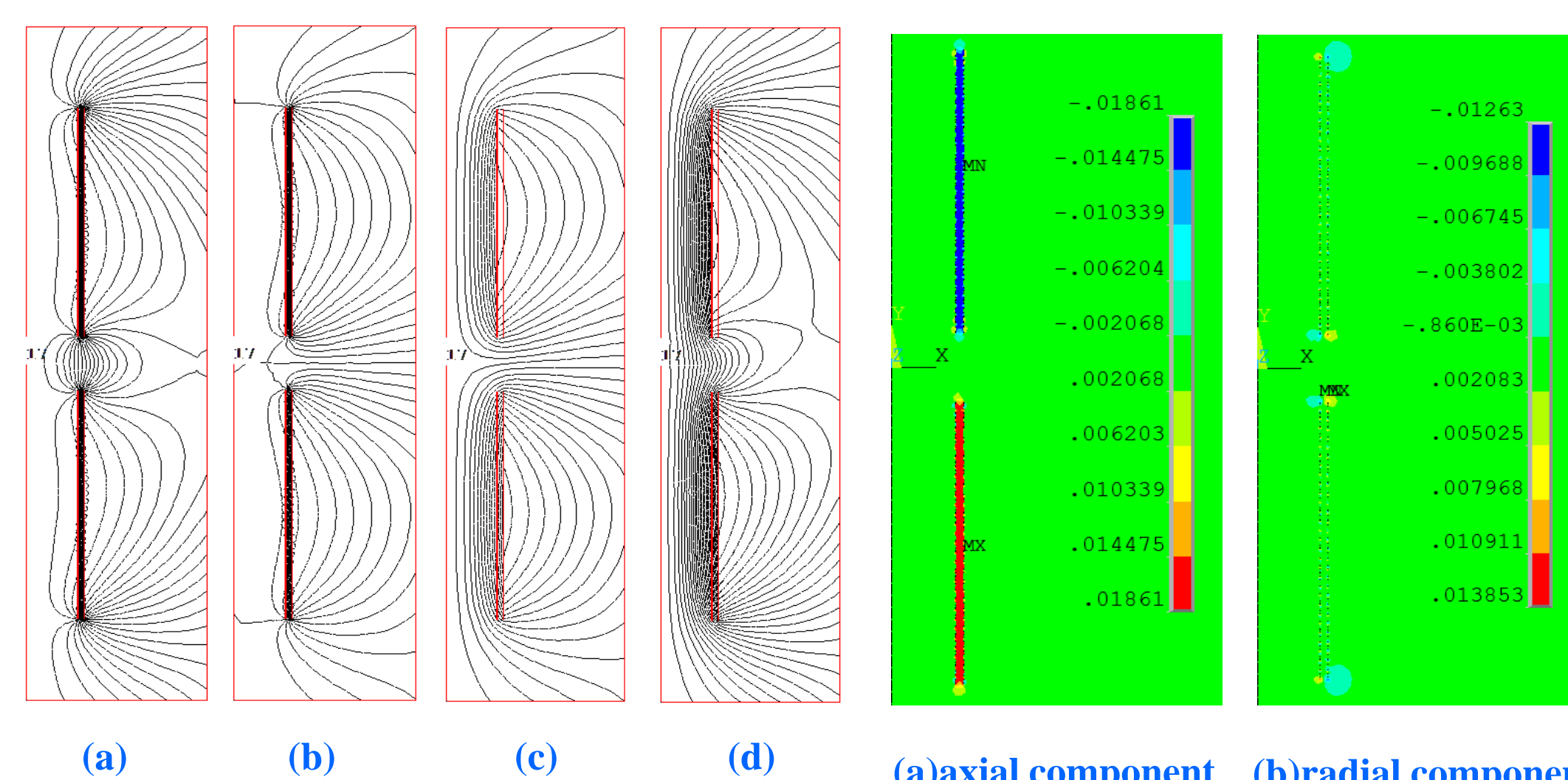


Fig. 4. Magnetic field lines of FC-SFCL. (a) double-branch operation for scheme 1; (b) double-branch operation for scheme 2; (c) single-branch operation for scheme 1; (d) single-branch operation for scheme 2.

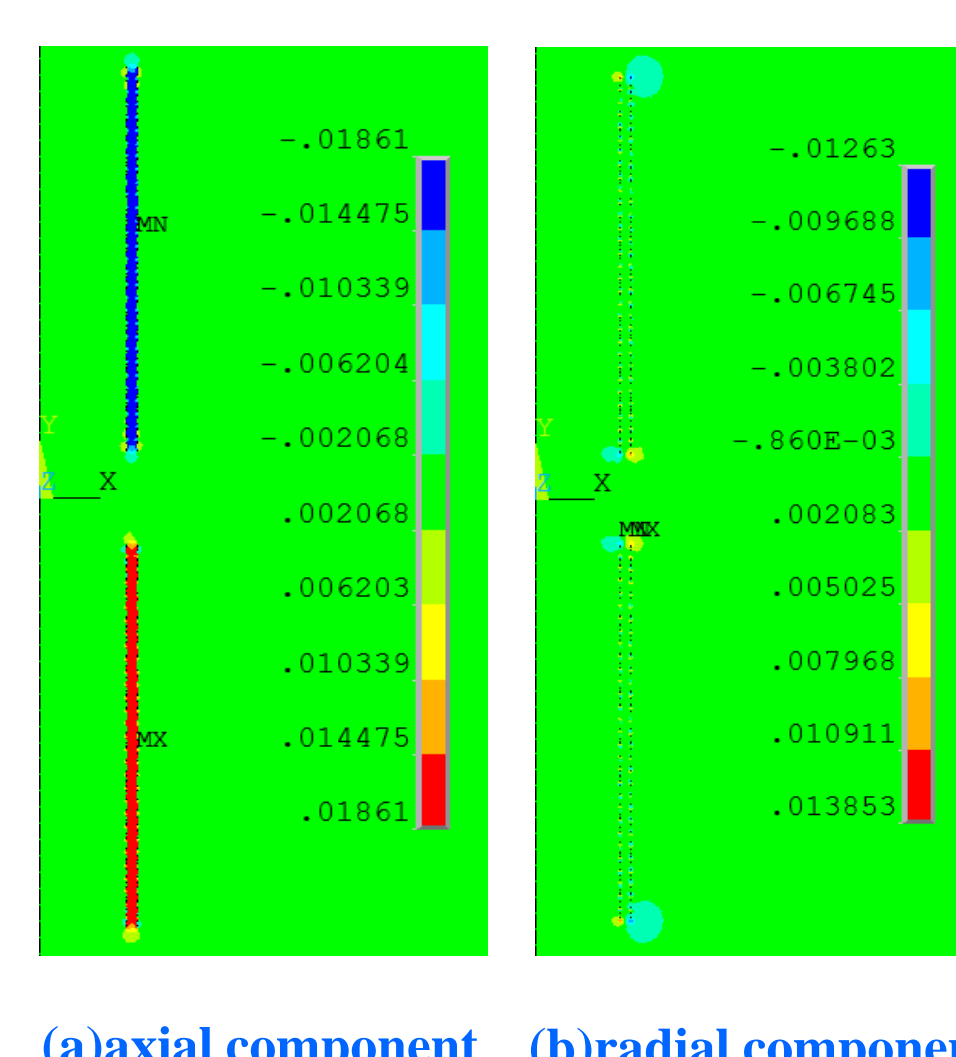


Fig. 5. Magnetic flux density distribution of FC-SFCL.

## SIMULATION OF IMPEDANCE PARAMETERS FOR SFCL

- The simulation model is built with MATLAB software. The DC voltage is 10 kV, normal current is 400A, and prospective DC fault current is 12kA.
- Different impedance characteristics exhibit at the beginning and end of current limiting process.

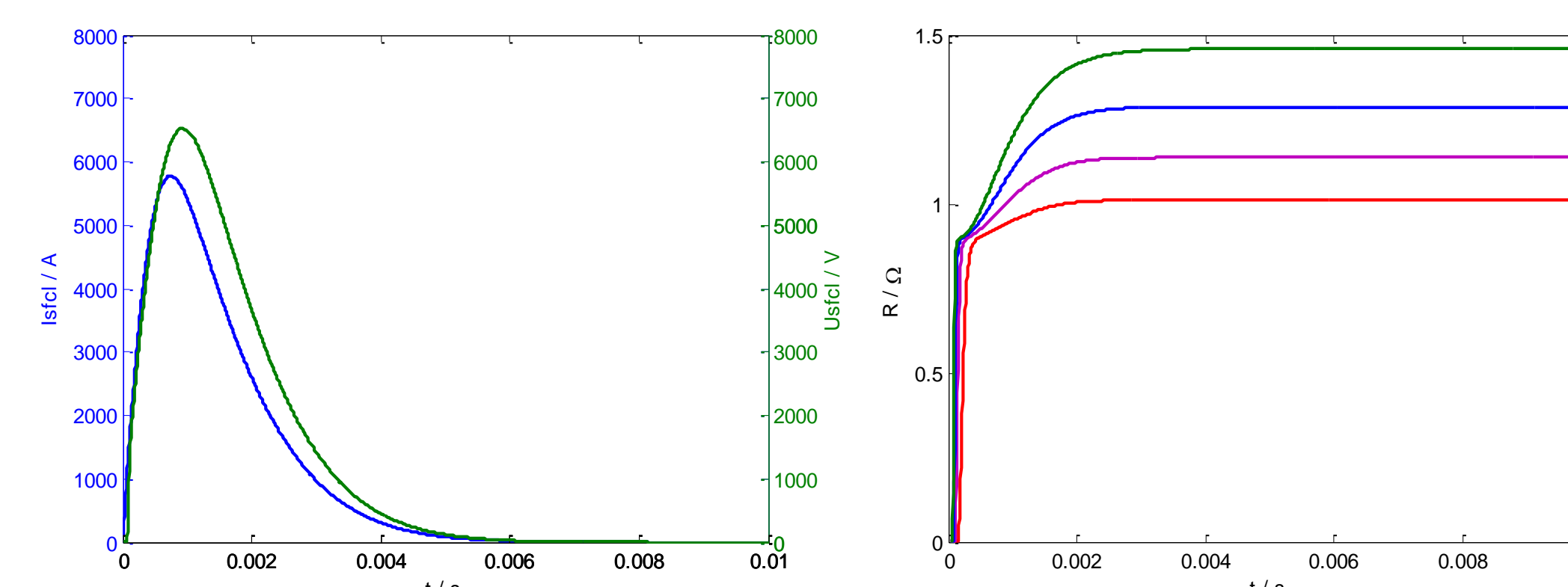


Fig. 6. Simulated voltage and current waveforms of DC FC-SFCL module (Voltage=10 kV, C=1mF, H=0.5mH).

Fig. 7. Simulated resistance characteristics curves of FC-SFCL module under different voltages (C=1mF, L=0.5mH).

- The dynamic simulation is established based on the RLC discharge equation.

$$(L_{\text{line}} + L_{\text{fcl}})C \frac{d^2 u_{\text{dc}}}{dt^2} + (R_{\text{line}} + R_{\text{fcl}})C \frac{du_{\text{dc}}}{dt} + u_{\text{dc}} = 0$$

$$\text{If } R > 2\sqrt{L/C} \quad i = -\frac{U_0}{L(p_2 - p_1)} (e^{p_1 t} - e^{p_2 t})$$

$$\text{If } R < 2\sqrt{L/C} \quad i = \frac{U_0}{\omega L} e^{-\delta t} \sin(\omega t)$$

$$\rho = \begin{cases} 0 & (J < J_c, T < T_c) \\ \rho_c (J/J_c)^{n-1} & (J > J_c, T < T_c) \\ f(T) & (T > T_c) \end{cases}$$

## FABRICATION AND TEST OF SFCL MODULE

- Using AMSC Type 8602, two solenoid coils were fabricated. And then, the current-carrying ability of two coils is measured by traditional four probe method. The critical currents are higher than 260 A at 77 K.
- The current limiting characteristic of SFCL module is tested by a dc pulsed power supply. By setting the values of capacitor, reactor and resistance, and the voltage of capacitor, the SFCL module could be tested.

TABLE IV Test results of one FC-SFCL module

	No. 1	No. 2
Resistance per unit length / $\Omega \cdot \text{m}^{-1}$	0.125	0.125
Length / m	15.5	19
Room temperature / $\Omega$	1.94	2.38
Inductance / $\mu\text{H}$	60	60
Critical current / A	262@1 $\mu\text{V}/\text{cm}$	261@1 $\mu\text{V}/\text{cm}$
N value	39.5	41.5
Peak withstand current / A	> 10 Ic @ 10 ms for short sample	

Fig. 9 Schematic circuit diagram of the pulsed-dc power supply



Fig. 10 Photograph of pulsed-dc power supply and FC-SFCL module.

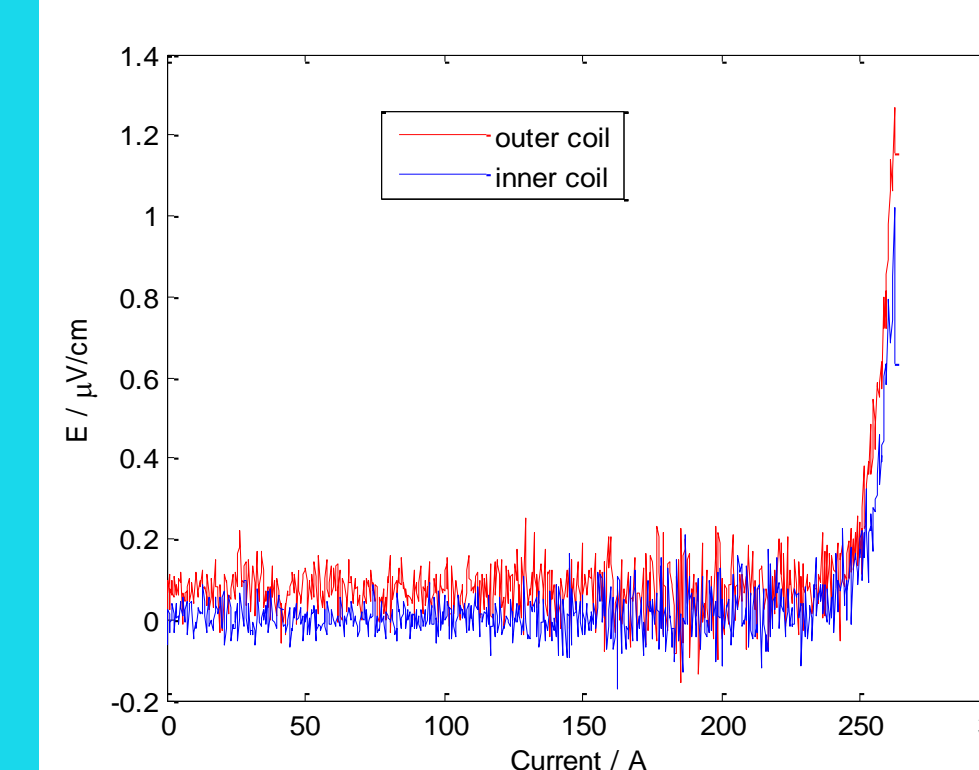


Fig. 8 The critical current test results of two coils

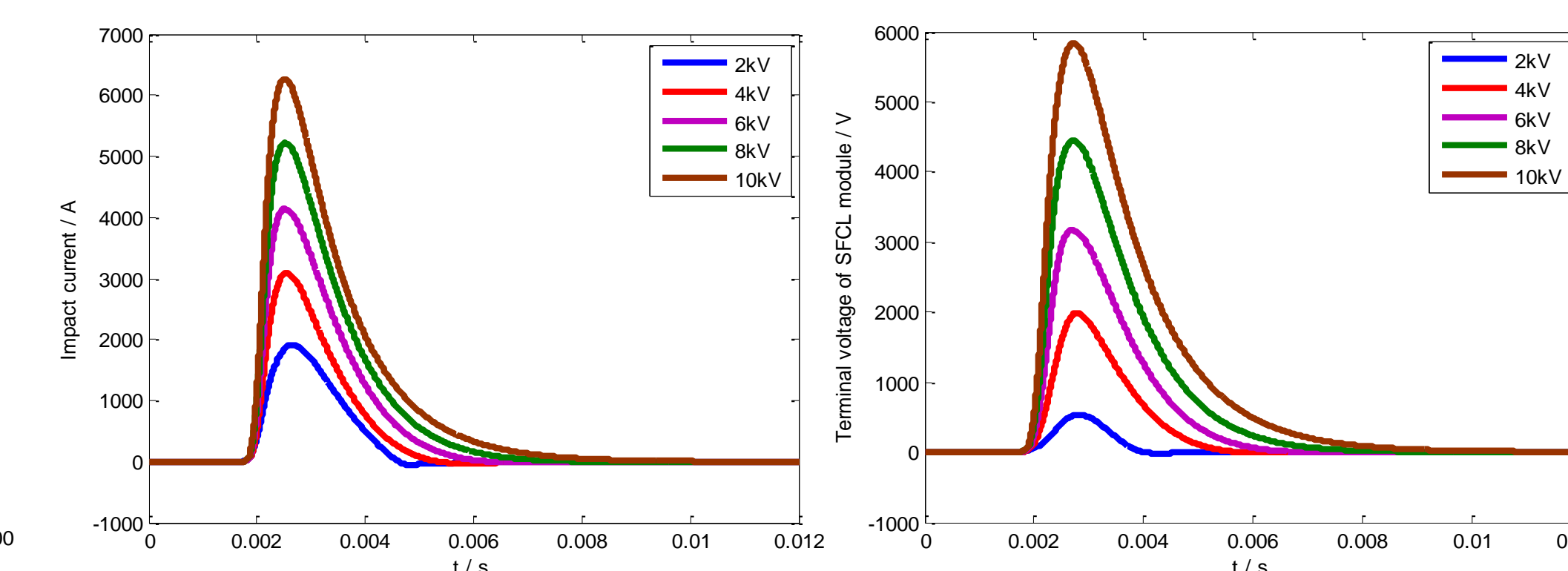


Fig. 11 The impact current and terminal voltage test results of SFCL module.

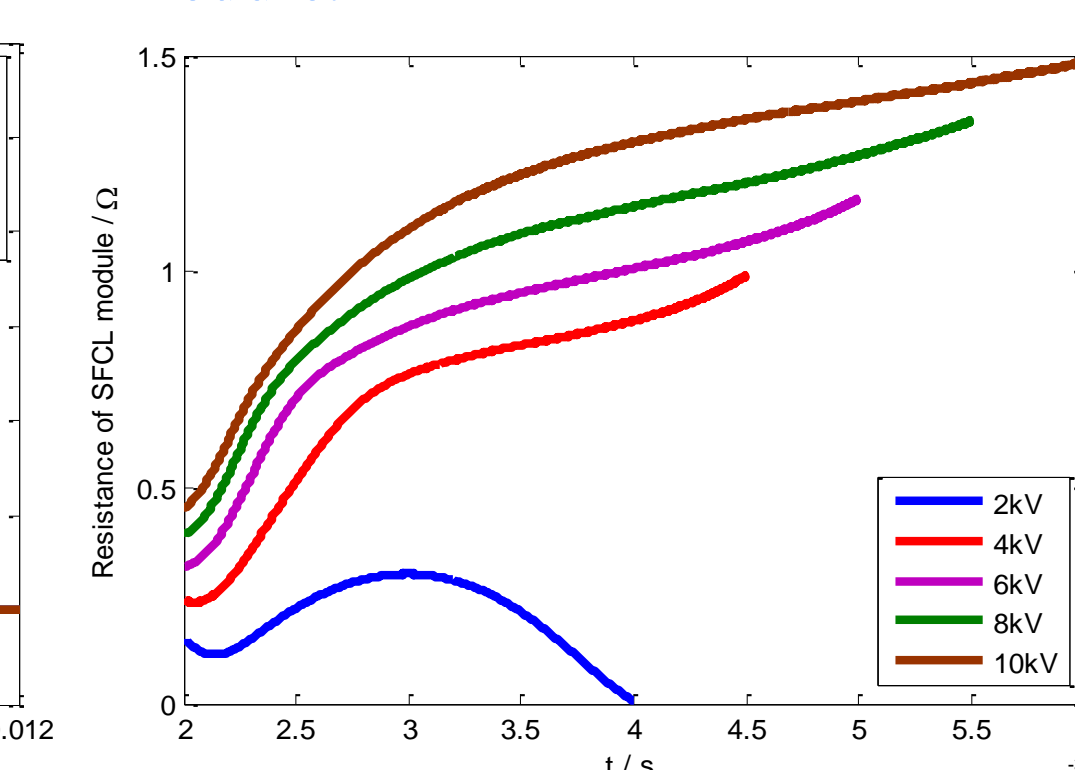


Fig. 12 The resistance test results of SFCL module.

- According to the measurement results, the maximum impact current of the superconducting coil could be limited from 12kA to 6264A when the dc impact voltage is 10kV, and the maximum terminal voltage can reach 5844V.
- According to the voltage and current waveforms, the resistance of SFCL module could be calculated. The largest resistance of SFCL module is about 1.5  $\Omega$  under 10 kV impact, which is close to the simulation results.

## ACKNOWLEDGEMENTS

This work is supported by National Key Basic Research Program of China (973 Program) (2015CB251005), Frontier Science Key Research Program of Chinese Academy of Sciences (QYZDJ-SSW-JSC025), and National Natural Science Foundation of China (No.51577179).